



Flume model test on the behavior of debris flows into the reservoir and the impact pressure acting on the dam embankment

Yusuke Sonoda¹ · Yutaka Sawada¹

Received: 17 April 2024 / Revised: 18 July 2024 / Accepted: 20 July 2024
© The Author(s) 2024

Abstract

The number of cases of damage to reservoirs due to debris flows has increased. In this study, granular material was released down the slope in a flume model to observe the debris flow morphology in a reservoir and to examine the impact pressure on a model dam embankment. The model flume had a slope angle of 30°, slope section width of 300 mm, and reservoir section width of 800 mm, and a model embankment with pressure and water pressure gauges was installed. Several experiments were conducted by varying the grain size of the granular materials to 3, 6 mm, mixed, and initial water storage levels. Observations from a high-speed camera indicate that when the debris flow enters the reservoir, the momentum rapidly decreases immediately after inflow. However, a solitary wave was generated, with heights reaching up to 2.5 times the initial water level. Additionally, during the impact of the debris flow on the model embankment, a large impact pressure was instantaneously generated. The magnitude and frequency of the occurrence tended to be more pronounced when the grain size was large. Additionally, the instantaneous impact pressure reached approximately twice the average impact pressure. However, with the exception of instantaneous large impact pressures, the existing equations used in the design of Sabo dams and coefficients with a specific range proposed in previous studies can be used to successfully calculate the impact pressure acting on the embankment in relation to the velocity.

Keywords Debris flow · Fill dam · Impact pressure · Model test

Introduction

Extreme weather events associated with climate change increase the frequency and damage due to debris flows owing to landslides and hillslope failures, seriously impacting structures and human life (IPCC 2023; Gariano and Guzzetti 2016). Small-scale fill dams that store water for agricultural use are often built in valleys or on steep slopes where water accumulates. Therefore, they are most seriously affected by debris flows. For example, in Japan, there are more than 150,000 small fill dams, termed as "Tameike", that store water for agricultural use (Ministry of Agriculture, Forestry and Fisheries 2024). In recent years, many cases have been reported in which debris flows or large amounts

of sediment from upstream areas have caused fill dams to collapse. This in turn led to damage in downstream areas (Shoda et al. 2016). Safety assessments have been performed for earthquakes, floods, and leakages in many fill dams. However, they have not been performed for debris flows. Potential debris flow risks include the overtopping of inflow-generated waves and destruction of the dam embankment and ancillary structures caused by the impact. However, the lack of specific methods and findings for evaluating these risks implies that the safety against debris flows cannot be evaluated.

Previous research on debris flows and landslide masses entering a body of water include studies on the development and reach of tsunamis generated when debris flows and landslides enter large dam sites. For example, Miller et al. (2016) conducted a detailed study of tsunami height, velocity, and morphology, as well as run-up heights and sediment geometry in the far-field region when a landslide impacts water using a relatively large experimental flume and simulated debris flow (ceramic beads). Bullard et al. (2023) quantitatively evaluated the mobility of debris

✉ Yutaka Sawada
sawa@harbor.kobe-u.ac.jp

Yusuke Sonoda
sono@boar.kobe-u.ac.jp

¹ Graduate School of Agricultural Science, Kobe University,
1-1 Rokkodai, Nada-ku, Kobe, Hyogo 657-8501, Japan

flow landslides using a similar experimental setup. Their research aimed to realize a more precise simulation of debris flows and elucidate the impact of mobility on the generated impulse waves. Additionally, Fritz et al. (2004) examined the characteristics of impulse waves in detail near fields by controlling a number of characteristics of inflow debris flows. Similar experiments have been conducted at different scales and with various granular materials, including studies using ceramic beads as described above, actual soil (Okura et al. 2002), solid blocks to investigate tsunami heights (Heller and Spinneken 2013; Sælevik et al. 2009), or using bagged granular materials (Evers and Hager 2015). Additionally, several studies have been conducted to elucidate the mechanism and behavior of debris flows (Bowman et al. 2009; Bryant et al. 2015; Iverson and Denlinger 2001). Iverson (2015) conducted almost real-scale debris flow experiments and discussed the influence of scale effects and boundary conditions on real phenomena and model experiments. Although the target was not debris flows, several studies have been conducted on impulse waves caused by snow avalanches, which have a lower density than landslides, similar to the study by Zitti et al. (2016). Many studies including numerical study have long been conducted in the field of dams installed on slopes as facilities to protect against debris flows (referred to as Sabo dams), most of which have focused on the impact pressure exerted by debris flows on dams and shape of the sedimentation (Miyoshi and Suzuki 1990; Shimoda et al. 1993; Zhou et al. 2019).

However, small-fill dams for irrigation, which are the subject of this study, differ significantly in their characteristics from the large dam sites and Sabo dams described above. First, earthen embankments and ancillary facilities have lower strengths than concrete structures. Additionally, the distance between the point of inflow of the debris flow and dam embankment is short; therefore, there is a high possibility that the debris flow will physically impact the dam embankment. Based on this point of view, it is essential to identify the risk of overflow and impact pressure at the time of debris flow inflow to evaluate the safety of facilities. However, there is a paucity of studies on these facilities with the exception of the studies by Shoda et al. (2021, 2024). In these studies, useful information was obtained on the loading exerted on embankments by debris flows using experimental flumes. However, the behavior and impact pressure of debris flows during inflow have not been fully clarified because of the limitations of the experimental flume geometry (uniform flume width for the slope and reservoir). In addition, the water storage area where the water is located and the effect of the reservoir water-level have not been examined.

In this study, model tests were conducted in an experimental flume with a widened reservoir area at several water levels and granular materials to investigate the behavior of debris flows at the inflow, particularly the wave heights

generated and the effect of water storage on the momentum-reducing effect of debris flows. Furthermore, the impact pressure due to debris flows was measured, and the applicability of the existing equations used in the design of the Sabo dam to a fill dam with water storage was examined.

Experimental method

Experimental equipment

Experimental flume

The experiment is conducted using an acrylic experimental flume, as shown in Fig. 1. A schematic of the experimental apparatus is shown in Fig. 2. The experimental flume consists of two sections: (i) a 3000-mm long and 300-mm wide slope inclined at 30°, and (ii) a 1000-mm long and 800-mm wide horizontal reservoir section with a model dam embankment installed in it. A polyvinyl chloride sheet covers the bottom of the slope and reservoir area. The granular material is released from the box in the upper part of the slope by manually opening the partition plate. Two laser displacement gauges are installed at intervals of 1500 mm on the slope flume (Fig. 2) to calculate the velocity at which the material flows into the reservoir based on the difference in reaction time.

Model dam embankment

The model dam embankment used in this experiment was made of solid polyvinyl chloride and fixed using bolts. As shown in Fig. 2, the upstream side of the model, where the debris flow impacts, has a slope structure similar to that of an actual dam embankment. The model is placed 300 mm

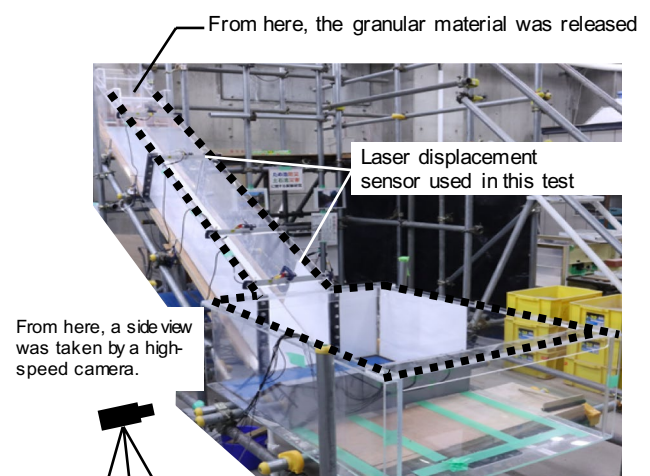


Fig. 1 Experimental flume

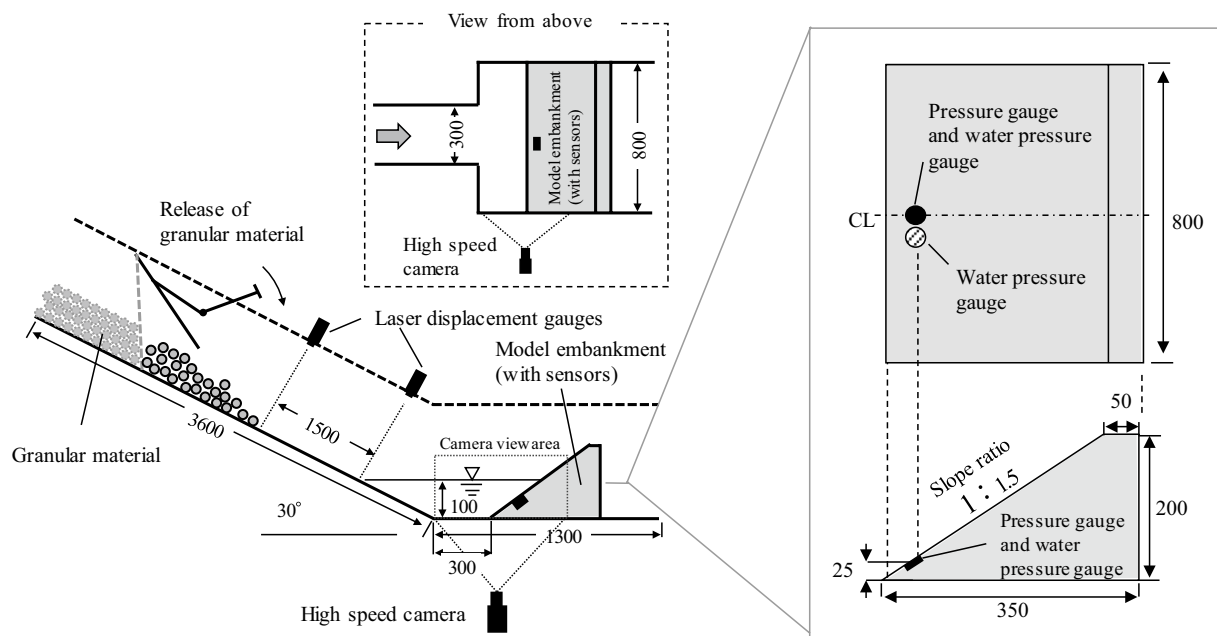


Fig. 2 A schematic of the experimental apparatus

away from the lower end of the slope. The specifications are as follows: height, 200 mm; base width (in the flow direction), 350 mm; crest width, 50 mm; length (in the perpendicular to flow direction), 800 mm; and slope ratio 1:1.5. In the embankment on site, the length is generally 4 to 15 times the height. In this experiment, the length of the model embankment is 4 times the height, which is not significantly different from the real embankment geometry. The slope ratio of the embankment was determined based on design guidelines (Ministry of Agriculture, Forestry and Fisheries of Japan 2015). Both pressure and water pressure gauges were installed at a height of 25 mm from the bottom of the centerline of the upstream slope of the model embankment (Fig. 2).

Granular material

Granular materials are spherical ceramic beads with a particle density of $\rho_s = 3.6 \text{ g/cm}^3$ and diameters of 3 mm (white), 6 mm (black), and 10 mm (red). Although ceramic beads have a larger particle density than ordinary soil, the flow velocity generally satisfies the similarity rule. Although the similarity rule is explained in the later section, the Froude similarity (Iverson 2015) rule was employed in this study. Also, the uniform particle size of the ceramic beads makes them an easy material for evaluating the effects of particle size. Three types of material were used for the debris flow, with a constant weight of 15 kg for all of the tests: a single particle size material of 3 and 6 mm, respectively, and a mixed particle size material of 3, 6 and 10 mm in the same

weight ratio. The volume of the material was $7.0 \times 10^3 \text{ cm}^3$. The granular materials were submerged in water before the experiment. Using a 3 mm or larger material eliminates the influence of the capillary effect, which is the attraction force between particles due to suction by water and allows conditions to be matched in each case (Take et al. 2016).

Experimental conditions

Experimental cases

Nine experimental cases were conducted; six cases displayed as d3_h0, d3_h50, d3_h100, d6_h0, d6_h50 and d6_h100, were conducted with a combination of three initial water levels of $h = 0 \text{ mm}$ (no water), $h = 50 \text{ mm}$, and $h = 100 \text{ mm}$ for each single grain size material ($d = 3 \text{ mm}$ and $d = 6 \text{ mm}$), and three cases displayed as dM_h0, dM_h50 and dM_h100, were conducted with three different initial water levels using a mixed particle size material of 3, 6 and 10 mm with the same mass (5 kg each). The case names for each condition are listed in Table 1.

Measurement

In this experiment, the impact pressure acting on the dam embankment during the inflow of debris is measured using pressure and water pressure gauges attached to the model dam embankment, as shown in Fig. 3. The values measured by the pressure gauges were classified into three categories: (i) impact pressure due to the granular

Table 1 Test cases

Case name	Granular material	Initial water height (mm)
d3_h0	3 mm (single)	0
d3_h50		50
d3_h100		100
d6_h0	6 mm (single)	0
d6_h50		50
d6_h100		100
dM_h0	3, 6, 10 mm (mix)	0
dM_h50		50
dM_h100		100

material itself, (ii) hydrostatic pressure variation due to water level fluctuations, and (iii) hydrodynamic pressure due to the movement of stored water. Given that the impact pressure due to granular materials affect the failure and deformation of the embankment and its ancillary structures (e.g., inclined conduits and gates), the impact pressure P due to the impact of granular materials was evaluated by subtracting the value measured by the water pressure gauge at the same location from the value measured by the pressure gauge.

$$P = p - u \quad (1)$$

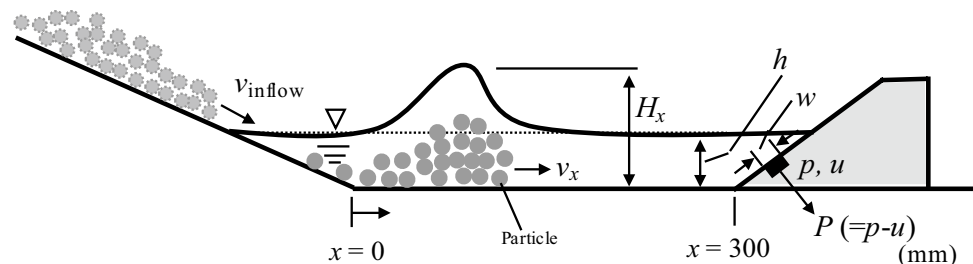
where P denotes the impact pressure owing to the granular material, p denotes the value measured by a pressure gauge, and u denotes the value measured by a water pressure gauge.

As shown in Fig. 3, the velocity v_{inflow} of the front edge of the debris flow immediately before flowing

down the slope and entering the reservoir was calculated based on the difference in the reaction time of the laser displacement gauges installed on the slope flume. Additionally, the debris flow behavior in the reservoir was captured using a high-speed camera (NAC Image Technology, Inc.). The frame rate was set to 2000 fps, and the shooting was synchronized with the measurement of the impact pressure. The velocity of submerged debris flow was measured using high-speed camera images. The bottom of the slope was set at $x = 0$ mm and x -axis increased toward the embankment model (Fig. 3). First, the number of frames captured by the high-speed camera was counted until the front edge of the submerged granular material reached $x = 50$ from 0 mm. Therefore, the velocity between $x = 0$ and 50 mm could be calculated using this counted frames, set frame rate and distance between $x = 0$ and 50 mm. This is defined as v_{50} . Similarly, the velocities from $x = 50$ to 100 mm were calculated as v_{100} , v_{150} , v_{200} , and v_{250} . As shown in Fig. 4, in the case of water storage, the front edge of the submerged granular material could be observed because it moved relatively uniformly. Conversely, in the case without water, the particles moved in separate pieces, and it was difficult to observe the front edge of a body. Therefore, a single particle was tracked, rather than tracking the front edge of the granular body.

Examination of the similarity rule

The geometric scale of the experiment was set to 1/20. According to Mizuyama (1979), the interparticle friction force, which is the most dominant force in the motion of sand-gravel-type debris flows, satisfies the Froude law. Furthermore, the equations for the momentum of the debris flow

Fig. 3 Measurements

- x : distance from slope end
- v_{inflow} : velocity of debris flow as it flows into the reservoir area
- v_x : velocity of debris flow in the reservoir area
- H_x : height of wave at x
- H_{max} : maximum value in H_x
- h : initial water height
- p : pressure measured by pressure sensor (perpendicular to the slope)
- u : water pressure measured by water pressure sensor
- P : impact pressure by granular material ($=p-u$)
- w : width (diameter) of the pressure gauge receiver surface

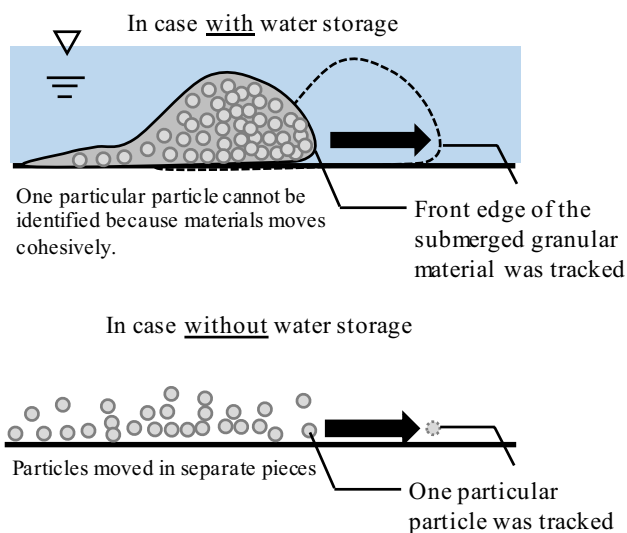


Fig. 4 Tracking point for calculating velocity of debris flow

also satisfy the Froude law. Therefore, in this experiment, the similarity rule for the Froude number (Iverson 2015), which is the velocity similarity rule, was considered in the model experiments. However, given that ordinary water is used in the reservoir, the Reynolds number, which is the ratio of inertial to viscous forces, is not the same for the prototype and model. Hence, it is smaller than that of the prototype, and the viscous force is relatively large.

The velocities of debris flows vary widely, and the average velocity of sand-gravel-type debris flows is generally estimated between 5.5 and 11 m/s (Ministry of Land, Infrastructure, Transport and Tourism 2008). In relatively mountainous upstream areas where the slope is steep, the velocity of debris flows is considered higher and velocities of

15 m/s have been measured (Prochaska et al. 2008; Murano 1965). Considering the 1/20 scale of the experiment, the velocity of the model, which satisfies the similarity rule, was 2.5–3.4 m/s. The velocities measured in this experiment were set 3.2–3.7 m/s, which will be described later. Although the velocities were slightly higher owing to the use of beads, they did not deviate significantly from the similarity rule.

Experimental results

Debris flow morphology observation

When a debris flow enters a reservoir, it is expected to reach the dam embankment with a thin profile and retain momentum in the absence of water storage. Whereas in the water storage, its behavior changes because of a certain amount of resistance. In this section, we focus on the changes in the morphology of the debris flow and generated waves. Figure 5 shows images of cases, d3_h100, d6_h100 and dM_h100, immediately after the inflow of debris flows until the time of impact on the dam embankment. Immediately after the inflow, the water surface was not significantly affected by the inflow of debris. No water droplets were scattered in all cases, thus maintaining the thin shape of the debris flow as it flowed down the slope. Subsequently, at the front edge of the debris flow, water entered the pore spaces between the particles, indicating that the shape of the debris flow changed as if it were swelling. Simultaneously, the water level gradually increased, forming a stable solitary wave. The expansion of the front edge immediately after inflow and formation of solitary waves were similar to those in the model experiment conducted by Miller et al. (2016). Figure 6 shows the relationship between the maximum water level of the solitary wave, H_{max} , and the

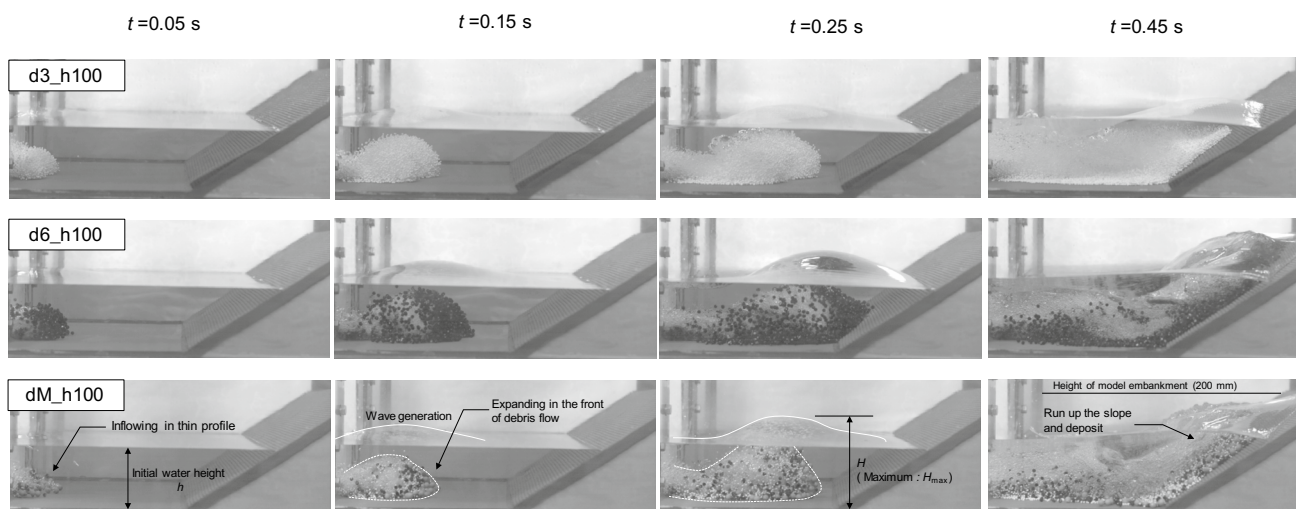


Fig. 5 Images of granular materials flowing into the water reservoir

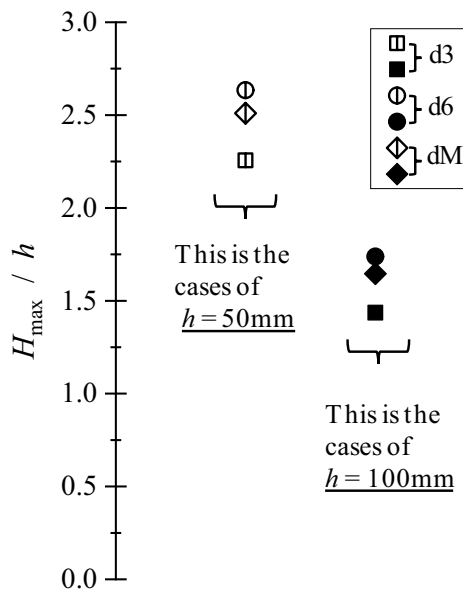


Fig. 6 H_{max}/h : Maximum wave height relative to initial water height

initial water level, h . The ratio of water level rise is 2.3–2.6 times for the $h=50$ case and 1.4–1.7 times for the $h=100$ case. These results indicate that the rate of increase in the wave height tends to be greater when the initial water level is low. Although a more careful discussion is required for a quantitative evaluation, this implies that even if the water level is low, the inflow of debris flows may cause the water level to rise significantly, increasing the risk of overflow if the embankment does not have sufficient freeboard.

Impact mitigating effect of stored water

Table 2 presents the leading-edge velocity of the debris flow at the lower end of the slope (before entering the reservoir). Cases d3 and dM exhibit approximately the same velocity, whereas d6 exhibits a slightly higher velocity. However, the difference is approximately 12%. Figure 7 shows the reduction ratio of velocity, which is defined as the reduction ratio of velocity v_x in the horizontal section to velocity v_{inflow} at the inflow in each case. The horizontal axis indicates the distance from the lower end of the slope (Fig. 3).

In the case of no water storage, the debris flow reached the embankment with a slight velocity deceleration. Conversely, in the case of water storage, the velocity was significantly reduced to less than 50% immediately after inflow, indicating

Table 2 Inflow velocity of each case

	m/s	h0	h50	h100	Ave
d3		3.1	3.2	3.2	3.2
d6		3.8	3.8	3.6	3.7
dM		3.4	3.3	3.3	3.3

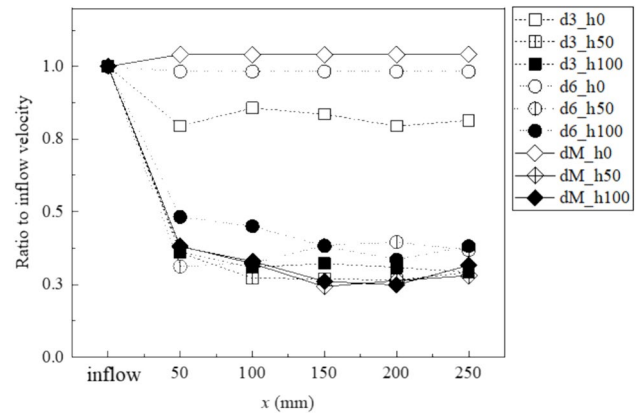


Fig. 7 Reduction ratio of debris flow velocity

that the impact-mitigating effect of the stored water was significantly enhanced. However, given that there was little difference between the initial water levels of 50 mm and 100 mm, it is considered that the momentum-reducing effect of water storage did not differ above a certain level of water storage. Comparing the reduction ratios for $x=200$ and 250 mm for cases with storage water in Fig. 7, d3 and dM are slightly smaller than d6, indicating a greater slow down. Figure 8 shows the particle deposition immediately after the experiment. The images on the left side of the figure shows the case with d3 particles, the center with d6 particles, and the right side with dM particles. The upper row of images shows the cases without water storage ($h=0$), and the lower row shows the cases with water storage ($h=100$). In the case with water storage, d3 particles (white) are deposited more upstream, whether the material of mixed (dM_h100) or single (d3_h100) particle size. Whereas in the case with d6 particles only (d6_h100), no such trend is observed. These results indicate that the momentum-reducing effect of the water storage was greater on the fine particles. Some experimental results (Bowman and Sanvitale 2009) show that the mobility of particle aggregations, such as debris flows, decreases with decreasing particle size below a certain value, but further investigation is required to clarify the mechanism in more detail.

Impact load

Calculation of load components due to granular materials

As explained in Eq. (1), the pressure measured by the pressure gauge included variations due to the water pressure. In previous studies (e.g., Shoda et al. 2024), loads were measured including both of the above. However, in the present study, only the impact pressure due to granular materials, which significantly contributes to the failure and deformation of dam embankments and ancillary structures, such as

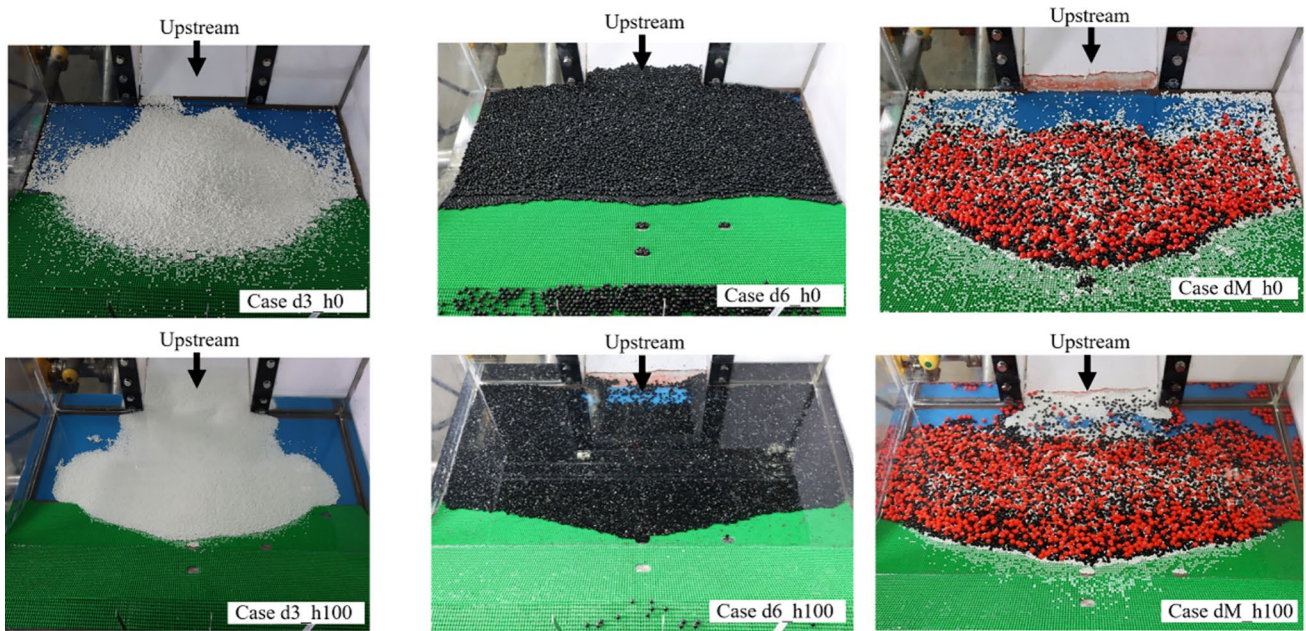


Fig. 8 Images of granular material deposition at $h=0$ mm and $h=100$ mm for each case

inclined flumes and gates, was evaluated by pressure. The impact pressure was evaluated by subtracting the value measured by the water pressure gauge at the exact location from that measured by the pressure gauge.

Figure 9 shows the change in impact pressure P over time (the value of the pressure gauge minus the value of the water pressure gauge) measured in each case. The data were low-pass processed with a threshold value of f based on Scheidl et al. (2013). The threshold value f was calculated as follows:

$$f = \frac{v}{w} \tag{2}$$

where f denotes the threshold value of the low-pass filter, v denotes the flow velocity of the granular material, and w denotes the width (diameter) of the pressure gauge receiver surface.

The change in the impact pressure due to the granular material over time showed a significant difference in the frequency of instantaneous large impact pressures between cases d3 and d6. In case d3, in which the grain size was 3 mm, such an instantaneous large impact pressure did not occur. Conversely, the frequency increased as the grain size increased. Fukuda and Fukuoka (2017) indicated that the instantaneous large impact pressure in debris flow disasters increases in frequency as the grain size increases, and this can occur in actual debris flows with the impact of huge stones and other objects. In the case of dM, where beads of three different grain sizes are mixed, the change and magnitude of the impact pressure are very similar to those in case d3 and instantaneous large impact pressures occur less

frequently. The behavior of a granular material consisting of a mixture of different grain sizes in the same mass is strongly influenced by the behavior of smaller grains. However, the magnitude of impact pressure with $h=0$ should be carefully discussed in each case. As shown in Fig. 7, the velocity immediately before the impact with the dam embankment differs by a factor of two or more between cases with $h=0$ and $h=50$ or 100 . Conversely, the magnitudes of the impact pressures were not significantly different. This may be due to the fact that in the case of no water storage ($h=0$), the momentum of the particles after impacting the embankment is too strong to be fully measured by the pressure gauges on the dam embankment slope as the particles bounce upward.

Based on the change in data over time, the maximum value of impact pressure, P_{max} , and the average of the top 30 impact pressures, P_{ave} , are extracted and discussed. These values are based on the data (250 data) between $t=0.25$ and 1.5 s when the graph in Fig. 9 generally rises. The change data over time generally consists of 6 to 8 data pieces per wavelength, and the top 30 averaged impact pressures should not be considered as instantaneous large impact pressures. Instead, they represent fluid forces that continuously act on and affect the dam embankment and its ancillary structures. Figure 10 compares P_{max} and P_{ave} for each case, and it can be observed that P_{ave} decreases slightly as the initial water level increases from $h=50$ to $h=100$. But the reduction rate is slight, indicating that the impact-mitigating effect of stored water above a certain level was small. Additionally, in the case of d3, the difference between P_{max} and P_{ave} is slight, whereas in the case of d6, P_{max} is almost twice the maximum value

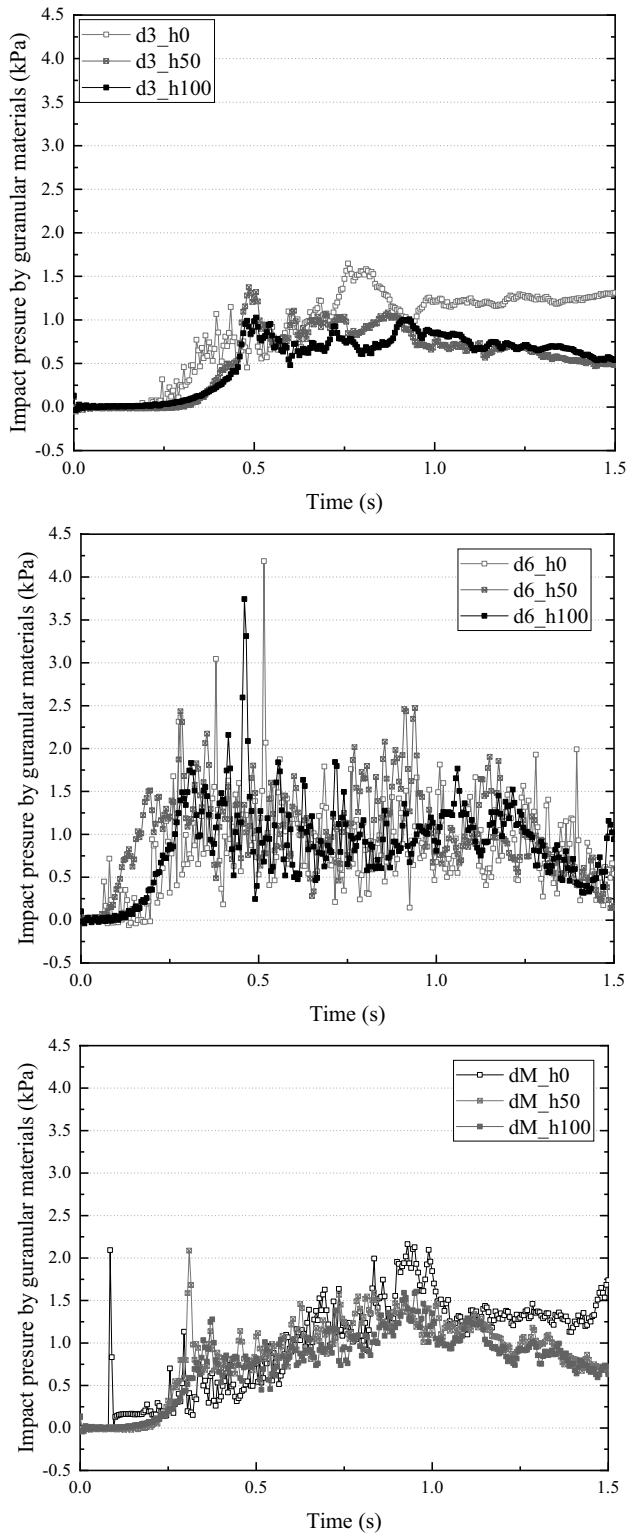


Fig. 9 *P*: Impact pressure by granular materials: The data were low-pass processed with a threshold value of *f* indicated in Eq. (2), referring to Scheidl et al. (2013)

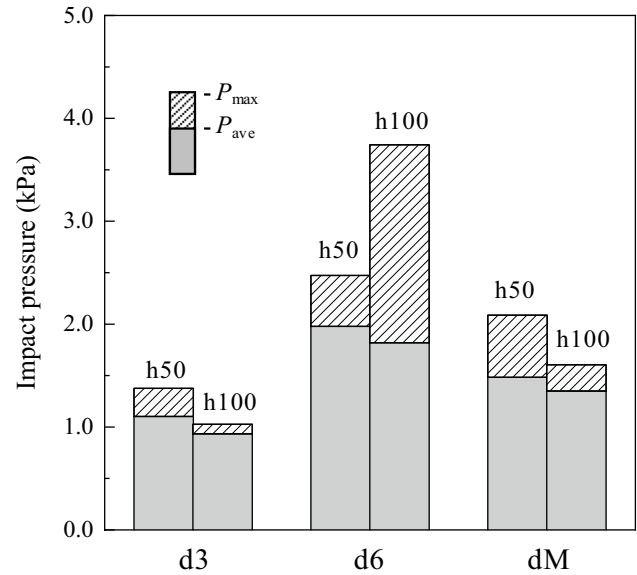


Fig. 10 Maximum impact pressure and average of top 30 data

of P_{ave} . Case dM exhibited intermediate values between those of d3 and d6. This indicates that large instantaneous impact pressures may be exerted regardless of water storage, depending on the form and type of debris flow.

Comparison with existing equations used in the design of Sabo dams

Based on the momentum of the fluid, the impact pressure P of the debris flow was calculated using Eq. (3), where the empirical coefficient α is proposed by various values based on experiments and field investigations and is known to have a certain range.

$$P = \alpha \cdot \rho \cdot v^2 \tag{3}$$

where v denotes velocity, ρ denotes the bulk density of the debris flow, and α denotes the coefficient. For example, Wendeler (2008) proposed a range for α from 0.7 to 2.0 based on impact pressure measurements obtained in laboratory experiments. Zhang (1993) proposed a range of α from 3.0 to 5.0 based on field measurements of over 70 actual debris flow sites. Furthermore, some studies also suggest $\alpha = 2.0$ for fine-grained materials (Watanabe and Ike 1981). In the design of Sabo dams for protecting against debris flows, the bulk density of debris flow, ρ , is calculated by the following Eq. (4) using the debris flow concentration, C .

$$\rho = \rho_s \cdot C + \rho_w(1 - C) \tag{4}$$

Although various values have been proposed for the earth flow concentration C (e.g., Takahashi 1978), the standard design for the Sabo dam (National Institute for

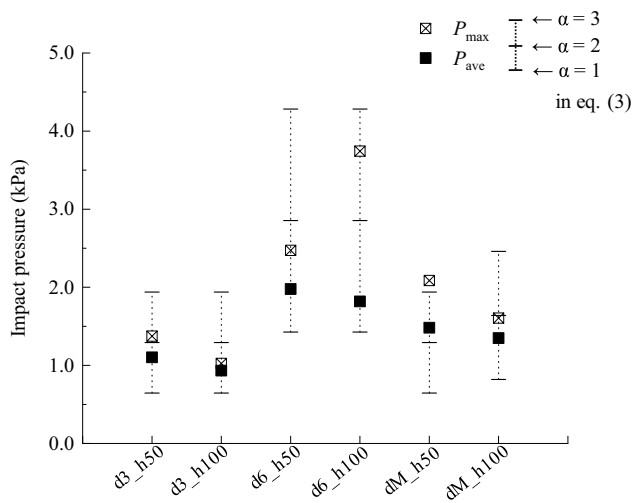


Fig. 11 Comparison of existing equations and experimental data

Land and Infrastructure Management, Ministry of Land, Infrastructure, Transport and Tourism 2016) generally states that it varies between 0.3 and 0.54 depending on the slope, with 0.3 for slopes of up to 10° and 0.54 for slopes of 16° or greater. Although a slope angle of 30° employed in this study is not assumed, the maximum value of $C=0.54$ was used. Concurrently, additional studies are required to determine how C should be set for behavior after inflow into the horizontal section.

Figure 11 compares the values of P_{\max} and P_{ave} measured in this experiment with those calculated using Eq. (3). As the measured pressure was perpendicular to the slope, P was calculated by substituting the velocity component perpendicular to the slope in Eq. (3). The lower and upper ends of the bars in the figure represent the values when $\alpha = 1.0$ and $\alpha = 3.0$, respectively. Furthermore, P_{\max} is plotted slightly above the bars in some cases, while P_{ave} is within the range of the bars between $\alpha = 1.0$ and 3.0 in many cases between $\alpha = 1.0$ and 2.0 . Hence, with the exception of instantaneous large impact pressures, the impact pressure exerted by a debris flow into a reservoir can be successfully calculated in relation to velocity by appropriately setting α , as suggested in previous studies.

Conclusion

In response to the increasing frequency of debris-flow disasters, model hydraulic experiments were conducted to investigate the behavior of the inflow of debris flows into fill dams located in valleys or on steep slopes, the momentum-reducing effect of water storage, and the impact pressure caused by granular materials. The following is a summary of our findings.

- (1) When a debris flow enters the reservoir, it rapidly reduces momentum immediately after the inflow. However, a solitary wave was generated, with heights reaching up to 2.5 times the initial water level.
- (2) Smaller grain sizes were more sensitive to the impact mitigation effect of stored water. However, no significant changes were observed above a certain water level.
- (3) The impact pressure on the dam embankment due to granular materials was instantaneous and large. However, the magnitude and frequency of the occurrence tended to be more pronounced when the grain sizes were large. The instantaneous impact pressure reached approximately twice the average impact pressure.
- (4) With the exception of instantaneous large impact pressures, the existing equations used in the design of Sabo dams and coefficients within a specific range proposed in previous studies can be used to successfully calculate the impact pressure acting on the embankment in relation to the velocity.

This study demonstrates the applicability of existing equations for calculating the impact pressure used in the design of Sabo dams and effects of water storage on debris flows into small-fill dams, which have rarely been studied. Furthermore, the influence of the scale of the experimental equipment and the use of ceramic beads as granular materials should be considered. For further clarification and quantitative evaluation of these phenomena, a numerical analysis using the results of this experiment as a benchmark is required.

Acknowledgements This study was supported by JSPS KAKENHI, Grant Numbers 21H02306 and 22KJ2235.

Funding Open Access funding provided by Kobe University.

Open Access This article is licensed under a Creative Commons Attribution 4.0 International License, which permits use, sharing, adaptation, distribution and reproduction in any medium or format, as long as you give appropriate credit to the original author(s) and the source, provide a link to the Creative Commons licence, and indicate if changes were made. The images or other third party material in this article are included in the article's Creative Commons licence, unless indicated otherwise in a credit line to the material. If material is not included in the article's Creative Commons licence and your intended use is not permitted by statutory regulation or exceeds the permitted use, you will need to obtain permission directly from the copyright holder. To view a copy of this licence, visit <http://creativecommons.org/licenses/by/4.0/>.

References

- Bowman ET, Sanvitale N (2009) The role of particle size in the flow behaviour of saturated granular materials. In: Proceedings of the 17th International Conference on Soil Mechanics and

- Geotechnical engineering, pp 470–473. <https://doi.org/10.3233/978-1-60750-031-5-470>
- Bryant SK, Take WA, Bowman ET (2015) Observations of grain-scale interactions and simulation of dry granular flows in a large-scale flume. *Can Geotech J* 52(5):638–655. <https://doi.org/10.1139/cgj-2013-0425>
- Bullard GK, Mulligan RP, Take WA (2023) Landslide tsunamis: exploring momentum transfer to waves generated by a range of materials with different mobility impacting water. *Landslides* 20:2619–2633. <https://doi.org/10.1007/s10346-023-02126-3>
- Evers FM, Hager WH (2015) Impulse wave generation: comparison of free granular with mesh-packed slides. *J Mar Sci Eng* 3(1):100–110. <https://doi.org/10.3390/jmse3010100>
- Fritz HM, Hager WH, Minor HE (2004) Near field characteristics of landslide generated impulse waves. *J Waterw Port Coast Ocean Eng* 130(6):287–302. [https://doi.org/10.1061/\(ASCE\)0733-950X\(2004\)130:6\(287\)](https://doi.org/10.1061/(ASCE)0733-950X(2004)130:6(287))
- Fukuda T, Fukuoka S (2017) Numerical movable-bed experiment on grain size segregation of debris flows and impacts on structures. *J Jpn Soc Civ Eng B1* 73(4):799–804. https://doi.org/10.2208/jscejhe.73.I_799
- Gariano SL, Guzzetti F (2016) Landslides in a changing climate. *Earth Sci Rev* 162:227–252. <https://doi.org/10.1016/j.earscirev.2016.08.011>
- Heller V, Spinneken J (2013) Improved landslide-tsunami prediction: effects of block model parameters and slide model. *J Geophys Res: Oceans* 118(3):1489–1507. <https://doi.org/10.1002/jgrc.20099>
- International Panel on Climate Change, IPCC (2023) Climate Change 2023 Synthesis Report Summary for Policymaker
- Iverson RM, Denlinger RP (2001) Flow of variably fluidized granular masses across three-dimensional terrain: 1. Coulomb mixture theory. *J Geophys Res: Solid Earth* 106(B1):537–552. <https://doi.org/10.1029/2000JB900329>
- Iverson RM (2015) Scaling and design of landslide and debris-flow experiments. *Geomorphology* 244:9–20. <https://doi.org/10.1016/j.geomorph.2015.02.033>
- Miller GS, Take WA, Mulligan RP, McDougall S (2016) Tsunami generated by long and thin granular landslides in a large flume. *J Geophys Res Oceans* 122(1):653–668. <https://doi.org/10.1002/2016JC012177>
- Ministry of Land, Infrastructure, Transport and Tourism (2008) https://www.mlit.go.jp/mizukokudo/sabo/dosekiriyuu_taisaku.html, Accessed 10 Mar 2024
- Ministry of Agriculture, Forestry and Fisheries (2024) https://www.maff.go.jp/j/nousin/bousai/bousai_saigai/b_tameike/index.html#tameiketoha, Accessed 10 Mar 2024
- Ministry of Agriculture, Forestry and Fisheries (2015) Guideline for design of irrigation reservoir in land improvement project. (In Japanese)
- Miyoshi I, Suzuki M (1990) Experimental study on impact load on a dam due to debris flow. *J Jpn Soc Erosion Control Eng* 43(2):11–19. https://doi.org/10.11475/sabo1973.43.2_11
- Mizuyama T (1979) Calculation of debris flow impact force on erosion control dam and its problems. *J Jpn Soc Erosion Control Eng* 32(1):40–43. <https://doi.org/10.11475/sabo1973.32.40>
- Murano Y (1965) On the Tokachidake mudflow. *J Jpn Soc Erosion Control Eng* 18(3):14–23. https://doi.org/10.11475/sabo1948.18.3_14
- National Institute for Land and Infrastructure Management, Ministry of Land, Infrastructure, Transport and Tourism (2016) Manual of technical standard for establishing sabo master plan for debris flow and driftwood. Technical Note of National Institute for Land and Infrastructure Management (904). (In Japanese)
- Okura Y, Kitahara H, Ochiai H, Sammori T, Kawanami A (2002) Landslide fluidization process by flume experiments. *Eng Geol* 66(1–2):65–78. [https://doi.org/10.1016/S0013-7952\(02\)00032-7](https://doi.org/10.1016/S0013-7952(02)00032-7)
- Prochaska AB, Santi PM, Higgins JD, Cannon SH (2008) A study of methods to estimate debris flow velocity. *Landslides* 5:431–444. <https://doi.org/10.1007/s10346-008-0137-0>
- Sælevik G, Jensen A, Pedersen G (2009) Experimental investigation of impact generated tsunami; related to potential rock slide. Western Norway, *Cost Eng* 56:897–906. <https://doi.org/10.1016/j.coastaleng.2009.04.007>
- Scheidt C, Chiari M, Kaitna R, Müllegger M, Krawtschuk A, Zimmermann T, Prose D (2013) Analysing debris-flow impact models, based on a small scale modelling approach. *Surv Geophys* 34:121–140. <https://doi.org/10.1007/s10712-012-9199-6>
- Shimoda Y, Suzuki S, Ishikawa N, Furukawa K (1993) Impact failure analysis of concrete check dam by distinct element method. *J Geol Eng* 480:97–106. [https://doi.org/10.2208/jscej.1993.480_97\(InJapanese\)](https://doi.org/10.2208/jscej.1993.480_97(InJapanese))
- Takahashi T (1978) The occurrence and flow mechanism of debris flow. *Soil Mech Found Eng* 26(6):45–50
- Take WA, Mulligan RP, Stevenson EP and Miller GA (2016) Physical modelling of landslides into reservoirs: effect of capillarity on rheology of granular landslide at impact. The part of Landslides and Engineered Slopes. Experience, Theory and Practice, pp 8
- Shoda D, Yoshisako H, Konno M, Inoue K, Suzuki H (2016) Survey of small earthfill dam damaged by debris flow due to concentrated heavy rain in August 2014. Technical report of the National Institute for Rural Engineering (218):65–76. (In Japanese)
- Shoda D, Yoshisako H, Kusumoto T, Inoue K, Kojima H (2021) Evaluation of the acting load for an irrigation reservoir at the time of inflow of the sediment. *Irrig Drain Rural Eng J* 89(2):371–378. https://doi.org/10.11408/jsidre.89.I_371
- Shoda D, Yoshisako H, Kusumoto T, Inoue K, Kojima H, Sakai N (2024) Evaluation of load against embankment due to debris flow flooded into agricultural reservoir stored water. *Irrig Drain Rural Eng J* 92(1):41–50. https://doi.org/10.11408/jsidre.92.I_41
- Watanabe M, Ike H (1981) Investigation and analysis of volcanic mud flows on mount Sakurajima, Japan. Erosion sediment transport measurement (Proceedings of the Florence Symposium), International Association on Hydrology, Florence, Science Publication (133):245–256
- Wendeler C (2008) Murgangsrückhalt in wildbächen. grundlage zur planung und berechnung von flexiblen barrieren. PhD thesis, Swiss Federal Institute of Technology Zurich, Zürich. <https://doi.org/10.3929/ethz-a-005699588>
- Zhang S (1993) A comprehensive approach to the observation and prevention of debris flows in China. *Nat Hazards* 7:1–23. <https://doi.org/10.1007/BF00595676>
- Zhou GGD, Du J, Song D, Choi CE, Hu HS, Jiang C (2019) Numerical study of granular debris flow run-up against slit dams by discrete element method. *Landslide* 17:585–595. <https://doi.org/10.1007/s10346-019-01287-4>
- Zitti G, Ancy C, Postacchini M, Brocchini M (2016) Impulse waves generated by snow avalanches: momentum and energy transfer to a water body. *J. Geophys. Res.: Earth Surface* 121(12):2399–2423. <https://doi.org/10.1002/2016jfo03891>